

Processing and characterisation of sol-gel glasses and powders in the system $\text{TeO}_2\text{-TiO}_2$

S. N. B. HODGSON, L. WENG

Institute of Polymer Technology and Materials Engineering, Loughborough University, Loughborough, Leicestershire, LE11 3TU, UK

E-mail: S.N.B.Hodgson@Lboro.ac.uk

Sol-gel processing routes have been developed for the production of thin films and powders in the system $\text{TeO}_2\text{-TiO}_2$ from tellurium and titanium alkoxides. The structure and properties of the resultant materials have been characterised as a function of heat treatment temperature. Pure sol-gel derived TeO_2 thin films are difficult to prepare with good optical transparency due to the presence of organic impurities and/or a highly dispersed metallic tellurium phase when heated at temperatures up to approximately 340°C , with crystallisation to $\alpha\text{-TeO}_2$ occurring when the heat treatment temperature is further increased. Additions of TiO_2 were found to retard the crystallisation of the $\alpha\text{-TeO}_2$ but promote the formation of other TiO_2 or TiTe_3O_8 phases. However, an optimum composition in the range $0.9\text{TeO}_2\text{-}0.1\text{TiO}_2$ was identified, which allows optically transparent thin films to be prepared with high refractive index and offers the potential for practical device manufacture. © 2002 Kluwer Academic Publishers

1. Introduction

Tellurite glasses are attractive for potential application to many technologies, such as, optical fibre amplifiers [1], ultraviolet-induced photo-refractive gratings [2] and new optical devices such as optical switches [3].

Some of the most promising of these optical materials are $\text{TiO}_2\text{-TeO}_2$ glasses [4] which are characterised by low glass transition temperature, high transmittance from the ultraviolet to near infrared region and good chemical durability plus high refractive index (n) and particularly non-linear refractive index (n_2). TiO_2 is known to be a highly effective additive for the purposes of increasing both n and n_2 in glass [5].

To date, most research into tellurite glasses has focused on conventional melting-quenching techniques [6–8]. However, the use of sol-gel processing techniques would be attractive for the low cost fabrication of thin films, coatings and waveguide type structures from these materials for use in practical optical and electronic devices. In addition, the sol-gel technique might be used for the fabrication of powders of these materials that could be subsequently formed into more substantive device structures by pressing and sintering techniques.

Earlier research by our group has demonstrated the feasibility of controlling the extreme reactivity of tellurium alkoxides by suitable, novel stabilisation approaches, allowing TeO_2 glasses to be fabricated in thin film form [9, 10]. However the limited thermal stability of such glasses, discussed in this work, poses real problems for the fabrication of such materials with the necessary transparency for optical device application.

This paper focuses on the possibility of extending the techniques developed for the sol-gel processing of TeO_2 for the fabrication of multicomponent $\text{TeO}_2\text{-TiO}_2$ thin films, with a view to improving the stability and developing a material more suited to optical device fabrication, and includes a discussion of the synthetic and fabrication procedures used for both powders and sol-gel coatings, the thermal stability and optical properties of the resultant materials, together with an investigation into the microstructure and other factors affecting the optical behaviour of these materials in thin film form.

2. Experimental procedure

2.1. Preparation of $\text{TeO}_2\text{-TiO}_2$ powders

and thin films from alkoxide precursors

To allow the effects of the modifying additives to be determined, this study comprised an investigation into both unmodified alkoxide systems, hydrolysis of which resulted in powder formation, and chemically modified alkoxides suitable for the production of thin films.

Powders of various compositions in the system $\text{TeO}_2\text{-TiO}_2$, were produced from a mixed alkoxide solution, containing the required proportions of alkoxide precursor in anhydrous ethanol to give a total molar concentration of alkoxide of 0.1 M. Tellurium ethoxide, $(\text{Te}(\text{OC}_2\text{H}_5)_4$ Inorgtech 99.9%) and titanium isopropoxide $(\text{Ti}(\text{OCH}(\text{CH}_3)_2)_4$: Koch Light >99%) were used as precursors. Additionally, TeO_2 powder was produced by the same route for comparative purposes. In each case, the alkoxide solution was hydrolysed by exposure to air, with the required water for hydrolysis

being supplied from atmospheric moisture. The solvent was allowed to evaporate at room temperature, with the resulting powders being retained for subsequent analysis/characterisation following heat treatment to various temperatures.

The production of thin films of various compositions in the system TeO₂-TiO₂, required the stabilisation of the alkoxide precursors to retard the hydrolysis and prevent precipitation of oxide particles. Stabilised solutions of the precursor alkoxides were separately prepared as follows:

- Under a glove box under dry nitrogen, tellurium ethoxide (Te(OC₂H₅)₄—Inorgtech 99.9%) was added to anhydrous ethanol to produce a 0.1 M solution. To this solution further additions of 10 vol% 1,2 propanediol (99% Aldrich) and 2 vol% Ethylene glycol (99%, Aldrich) stabilisers were made to give a total mole ratio of alkoxide: diols of approximately 1 : 30. The resultant solution was then refluxed for 1 hour at 80°C under argon.
- The titanium precursor solution was prepared by making stabilising additions of acetylacetonone (CH₃COCH₂COCH₃; 99.5%, BDH/Merck) to titanium isopropoxide to give an acetylacetonone : alkoxide mole ratio of 2 : 1. The mixture was refluxed at 90°C for 2 hours, then diluted to a 1 M solution with anhydrous ethanol.
- Finally, the Te(OPrⁱ)₄ and Ti(OPrⁱ)₄ solutions were mixed in the appropriate proportions to give a range of compositions from 2.5 to 35 mol% TiO₂ and further refluxed at 80°C for 1 hour under argon.

Thin films were made from the diol/acetylacetonone stabilised, mixed solutions after refluxing and cooling by dip-coating a previously cleaned and degreased glass substrate (Plain Micro Slides, Corning) at a withdrawal speed of 0.6 mm/sec. This was then placed in an oven at 120°C to produce the coating. The mechanism by which the TeO₂ based coating films are produced on heating is somewhat different to that in conventional sol-gel derived coatings and has been discussed in detail in a separate publication [10]. A similar process, but using only the stabilised tellurium ethoxide solution was also used to prepare thin films of TeO₂ for comparative purposes.

The resultant coated substrates obtained from these stabilised compositions were subsequently heat treated in air at various temperatures in the range 250–500°C for 30 minutes in a preheated furnace and used for optical and microstructural characterisation. The available XRD and thermal analytical techniques were not sufficiently sensitive to analyse the films *in situ*, and “bulk” samples for study by these techniques were therefore obtained by scraping the coating from the substrate prior to heat treatment and collecting the obtained material for analysis.

The coating thickness obtained from a single coating cycle was of the order of 0.03 μm

2.1.1. Optical characterisation

Optical characterisation was performed on those samples that exhibited suitable optical transparency after

heat treatment. This entailed determinations of refractive index (n), band gap (E_g) and Urbach energy (E_e).

To measure the refractive index of thin films, it was necessary to repeat the dip coating cycle, with intermediate heat treatment stages at 450°C, to build up the required coating thickness. A total of 15 dip coating cycles were used to give a total coating thickness of approximately 0.5 μm. The coating film on one side of the substrate was subsequently removed by swabbing with a 5% HCl solution, to allow refractive index measurements to be obtained from the interference effects observed over the wavelength range of 300–1100 nm using a Perkin-Elmer Lambda 2 double beam spectrophotometer according to the method of Swanpoel [11] from Equations 1 and 2.

$$n_{(\lambda_{M,m})} = [N + (N^2 - s^2)^{1/2}]^{1/2} \quad (1)$$

where

$$N = \frac{2s(T_M - T_m)}{T_M T_m} + \frac{s^2 + 1}{2} \quad (2)$$

and $n_{(\lambda_{M,m})}$: calculated refractive index value at a wavelength corresponding to an interference maxima or minima, T_M , T_m : maxima and minima of transmissivity respectively s : refractive index of substrate.

The band gap was calculated assuming that the absorption coefficient changes with frequency at the absorption edge according to the Equation 3 [12]:

$$\alpha(\omega) = \frac{B(\hbar\omega - E_g)^r}{\hbar\omega} \quad (3)$$

where $\alpha(\omega)$: the absorption coefficient at an angular frequency of $\omega = 2\pi\nu$, \hbar : $h/2\pi$, h : Planck's constant, $\hbar\omega$: photon energy (eV), B : a constant, r : an index which may have values of 2, 3, 1/2, and 3/2, depending on the nature of electronic transitions responsible for the absorption [13].

An indirect transition mechanism was assumed for these glasses in accordance with the findings of other studies [12, 14–17] on conventionally melted tellurite glasses, with a value of $r = 2$ thus used in Equation 1.

The value of E_g was obtained from the extrapolation of the linear region of a plot of $(\alpha/\omega)^{1/2}$ against photon energy to the point where $(\alpha/\omega)^{1/2} = 0$.

The Urbach energy (E_e), which describes the width of the band tails of the localised states in the normally forbidden band gap, was calculated from a plot of $\ln[\alpha(\omega)]$ vs ω (or $h\nu$) according to the relationship given in Equation 4 [16]:

$$\alpha(\omega) = \alpha_0 \exp(\hbar\omega/E_e) \quad (4)$$

where α_0 : a constant.

2.1.2. Microstructural characterisation

The microstructure of the thin films after heat treatment was observed by FEG-SEM. Samples were carbon coated to facilitate imaging.

2.1.3. Thermal stability

The process of thermal decomposition and/or crystallisation of the gel and particulate reaction products were also studied by thermal analysis using both DSC and TGA. Measurements were performed under air atmosphere using a Mettler DSC 30/TG 50 instrument. A temperature range 60°–580°C was investigated with a heating rate of 10°C/min.

These measurements were supported by X-ray powder diffraction experiments, following heat treatment to various temperatures up to 600°C, performed on both powder and “bulk” gel samples derived from coatings as outlined above, using a similar heating rate and atmosphere to those used in the thermal analyses.

3. Results and discussion

3.1. Hydrolysis reactions and stabilisation

Both tellurium ethoxide and titanium isopropoxide undergo rapid hydrolysis when exposed to normal atmospheric conditions when dissolved in ethanol. The powders obtained from this reaction were in each case white in colour and agglomerated. Typically, the powder particle size obtained from the single and multicomponent compositions was of the order of 0.5 μm . The powders were amorphous to x-ray prior to heat treatment (Fig. 1).

The stabilisation of tellurium ethoxide to control the hydrolysis and allow the formation of sol-gel coatings is ineffective with most common stabilising additives, and is achieved in this case via the formation of solid complex, which is subsequently remelted during the initial “drying” heat treatment at 120°C. This somewhat unorthodox stabilisation mechanism is discussed in some detail in other publications by the authors [9, 10].

The stabilisation of titanium isopropoxide by reacting with acetylacetone has been previously reported in a number of publications [18], and is widely used to control the hydrolysis of this precursor, for example in the synthesis of PZT. However, acetylacetone reacts adversely with tellurium alkoxide precursors such as the ethoxide used in this work, resulting in virtually instantaneous breakdown of the alkoxide and the formation of

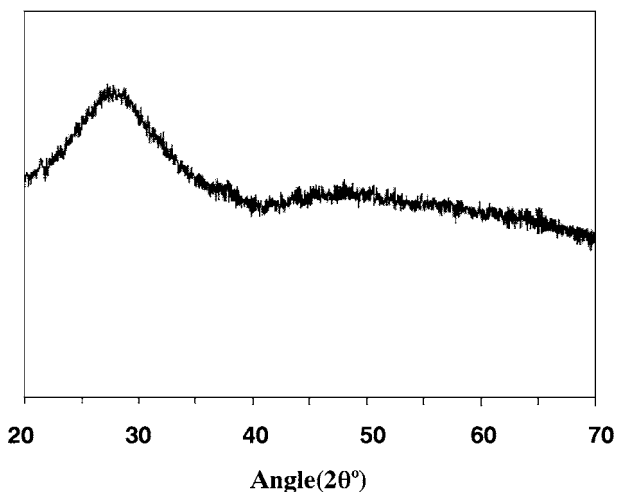


Figure 1 Typical XRD spectra of powder obtained from hydrolysis of the unstabilised alkoxides.

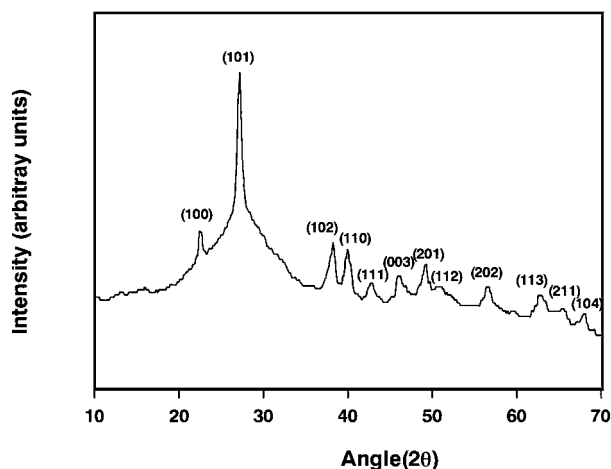


Figure 2 X-Ray spectra of the products obtained from reaction of tellurium alkoxide with acetylacetone (peak indexing as metallic Te structure).

metallic tellurium. A typical X-ray diffraction spectra obtained from the products formed from the reaction of acetylacetone with tellurium ethoxide is shown in Fig. 2. The peaks are indexed for metallic tellurium with hexagonal crystal structure [19].

Similarly, the reaction of $\text{Ti}(\text{OPr}^i)_4$ with diol is also deleterious to the properties of the resultant films in this system. $\text{Ti}(\text{OPr}^i)_4$ reacts with both ethylene glycol and 1,2 propanediol to form non volatile, solid complexes which are insoluble in alcohols and diols [20]. The precipitation of these insoluble complexes resulted in inhomogeneity, poor optical properties and early crystallisation of the TiO_2 phase when attempts were made to produce TeO_2 - TiO_2 coating films from diol stabilised alkoxides.

Consequently, the selection of appropriate addition levels and of the two stabilising additives, together with the appropriate sequence of stabilisation and mixing of the two precursors is critical to the success of this process route for TiO_2 - TeO_2 thin films.

The pre-reaction of the two alkoxides with their respective stabilising additives, via the refluxing process described in this work, thus ensures that each alkoxide is appropriately complexed to impart stabilisation whilst avoiding the adverse reactions described above.

The 2 : 1 mole ratio of acetylacetone to titanium isopropoxide used to stabilise this alkoxide ensures that no free acetylacetone is present after refluxing, but appears sufficient to impart stabilisation of this alkoxide towards hydrolysis. Acetylacetone is a stronger complexing agent than propanediol, and any excess acetylacetone not reacted with the titanium alkoxide precursor replaces the complexing diol species on the tellurium alkoxide species and results in the breakdown of the alkoxide as previously described.

Where the $\text{Ti}(\text{OPr}^i)_4$ is pre-reacted with acetylacetone in the correct stoichiometric ratio prior to mixing with the diol stabilised $\text{Te}(\text{OEt})_4$, then the formation of the Ti-diol complex, and the associated problems of phase separation, are prevented by the more strongly complexing character of the acetylacetone, with this Ti-acetylacetone complex being unreactive toward the diol.

3.2. Thermal stability and decomposition of alkoxide derived powder and gel products

DSC results obtained on heating the hydrolysed mixed alkoxide derived powder of various TeO₂-TiO₂ ratio are shown in Fig. 3, together with supporting x-ray diffraction results for samples of fixed composition as a function of temperature shown in Fig. 4 and as a function of composition at a fixed temperature in Fig. 5 respectively.

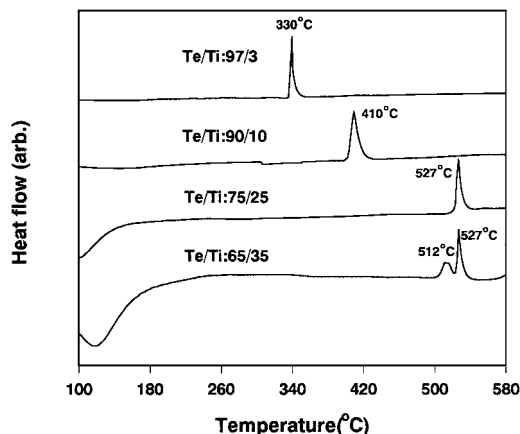


Figure 3 DSC curves of hydrolysis products from Te(OPr)₄ and Ti(OPr)₄ solution with different Te/Ti ratio.

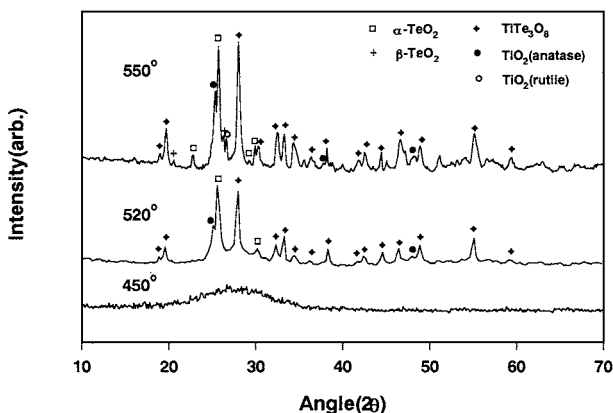


Figure 4 XRD spectra of hydrolysis products with Te/Ti = 65/35 after heat treatment at 450°C, 520°C and 550°C.

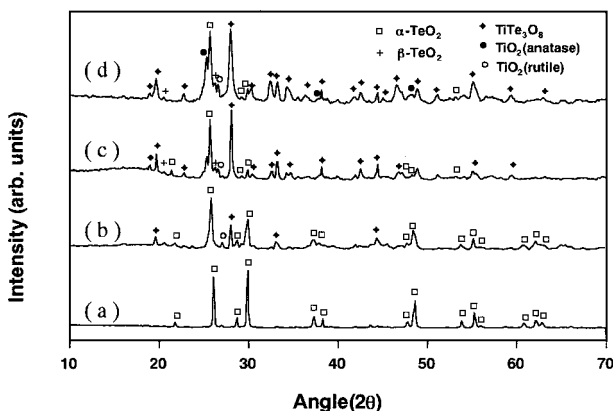


Figure 5 XRD spectra of hydrolysis products with Te/Ti mole ratio = (a) 97/3, (b) 90/10, (c) 75/25 and (d) 65/35 after heat treatment at 600°C for 30 minute.

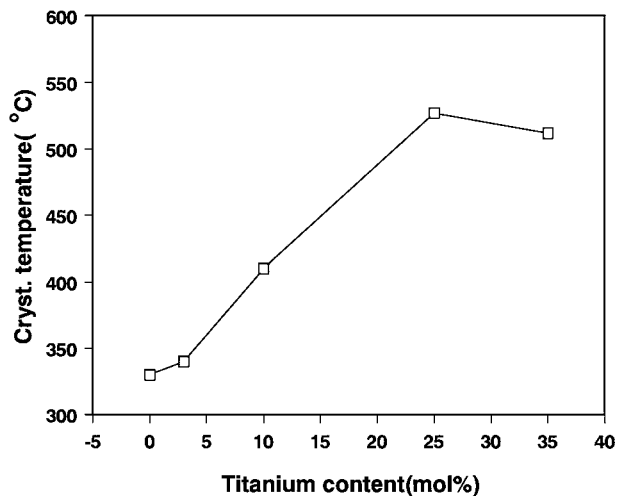


Figure 6 Influence of Te/Ti mole ratio on crystallisation temperature of powders derived from unstabilised alkoxide precursors.

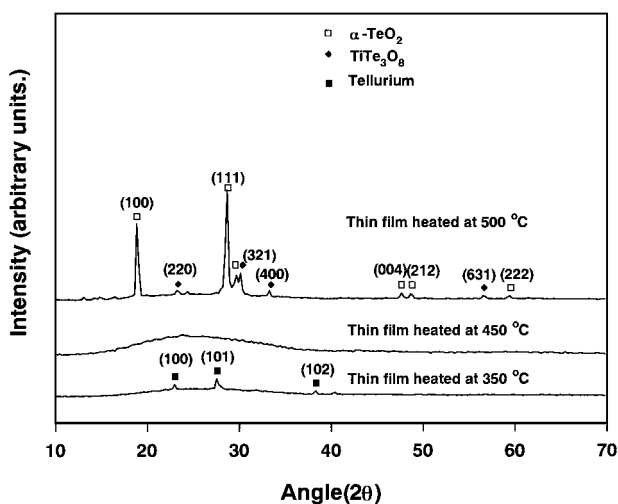
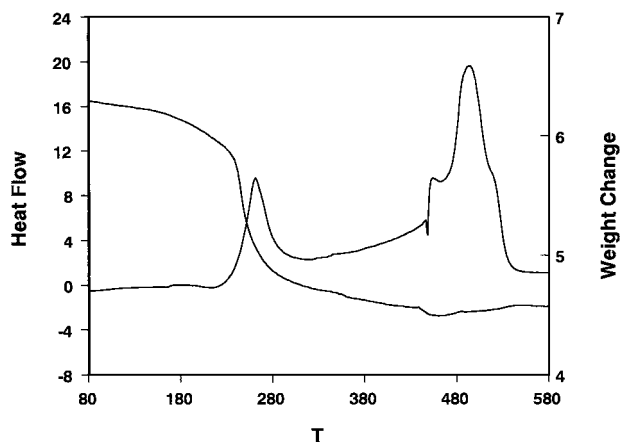


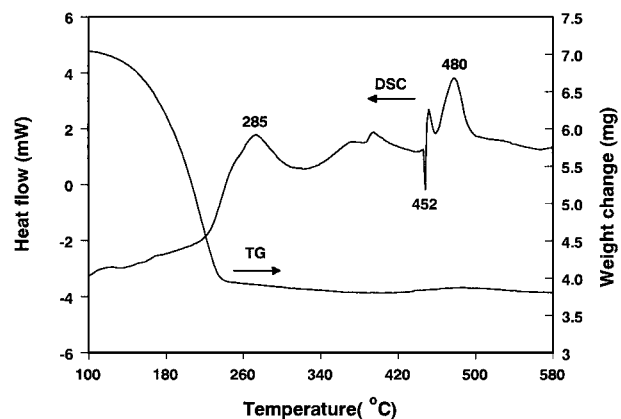
Figure 7 XRD pattern of 0.9TeO₂-0.1TiO₂ gel after heat treatment at 350°C, 450°C and 500°C.

These results indicate that increases in the TiO₂ concentration of the powders results in an increase in the crystallisation temperature, by approximately 200°C as the TiO₂ content is increased from 3 to 25 mol% (Fig. 6). In the case of samples of low TiO₂ content, crystallisation of α-TeO₂ occurs, with crystalline TiTe₃O₈, β-TeO₂ (minor component), anatase and rutile phases being successively formed as the TiO₂ content and/or temperature are increased.

Heat treatment of the coating films derived from the diol/acetylaceton stabilised mixed alkoxide solution produced somewhat different behaviour as illustrated by the XRD and thermal analysis results in Figs 7 and 8a. In the case of coatings containing up to 10 mol% TiO₂ addition, the sequence of events occurring on heat treatment is generally similar to that previously reported for TeO₂ thin films, but with the onset temperatures shifted. Data for the TeO₂ system is shown in Fig. 8b for comparison. At temperatures in the range approximately 240–320°C, a reduction reaction takes place resulting in the formation of nanoscale metallic tellurium precipitates evidenced by the appearance of the characteristic peaks for hexagonal Te in the XRD spectra, and a corresponding exothermic event



(a)



(b)

Figure 8 (a) Thermal analysis results for 0.9 TeO₂-0.1 TiO₂ gels derived from stabilised alkoxides. (b) Thermal analysis results for TeO₂ gels derived from stabilised alkoxides.

in the DSC results (Figs 4 and 5). At temperatures above approximately 320°C this phase begins to oxidise, characterised by an exothermic event in the range 320–450°C, with any residual metallic phase melting and rapidly oxidising above 450°C, characterised by a sharp endotherm and exotherm at 452°C and 460°C respectively. The intensity of the x-ray diffraction peaks for metallic Te are also reduced over this temperature range providing confirmatory evidence of this oxidation.

Additions of more than 10 mol% TiO₂ to TeO₂ in these stabilised systems produced quite different behaviour to that of the powders derived from the unstabilised system, with crystallisation of the TiO₂ component, as anatase, occurring at approximately 375°C, which prevented the fabrication of optically transparent thin films.

Comparing the behaviour of the TeO₂ and TeO₂-TiO₂ systems (Fig. 8a and b), the most significant effect of the TiO₂ addition is to suppress the formation of α-TeO₂, which occurs as a result of the oxidation of the metallic Te formed at temperatures as low as 360°C in the pure TeO₂ system [10]. In the case of the coating film of composition 90 mol% TeO₂-10 mol% TiO₂, oxidation of the metallic Te formed at low temperatures results in the formation of an amorphous product, presumably due to the dissolution of TiO₂ into this newly formed phase. Subsequent crystallisation (an exothermic event in Fig. 8a) does occur at temperatures

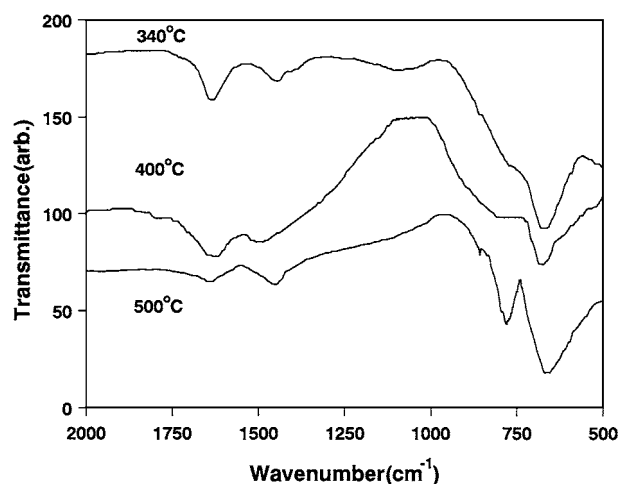


Figure 9 FTIR spectra for 0.9 TeO₂-0.1TiO₂ coating films after heat treatment at 320°C, 400°C and 500°C.

above approximately 480°C, primarily to α-TeO₂, with smaller amounts of TiTe₃O₈ as shown in the XRD results in Fig. 7.

In the case of those materials containing more than 10 mol% TiO₂ addition, the crystallisation of the TiO₂ components at low temperatures can be attributed to the chemical segregation associated with the formation of the metallic Te, resulting in the concomitant formation of TiO₂ rich regions. The formation temperature for the anatase phase is lower in this system than normally observed in pure sol-gel derived TiO₂ films [21], and is most probably due to the Te crystallites formed in this system acting as nucleation sites for the crystallisation of the TiO₂.

The results of the FTIR studies carried out on the variously heat treated stabilised gels are shown in Fig. 9. Over the temperature range 320–500°C the broad absorption band in the range 560–700 cm⁻¹ associated with the Te–O bond [12, 22, 23] initially develops a shoulder at around 750 cm⁻¹ which gradually increases in intensity and wavenumber to ≈780 cm⁻¹. These changes can be attributed [24] to the initially short-range ordering and subsequent crystallisation of TeO₂ with increasing heat treatment temperature.

The effect of heat treatment on the nano and microstructure of the TiO₂-TeO₂ thin films prepared in this work are shown in Fig. 10a–c after heat treatment at 300°C, 450°C and 550°C respectively. Fig. 10a shows the nanoscale crystallites of metallic tellurium formed at low temperatures, whilst the (nano) particulate nature of the films obtained after heating to 350°C is shown in Fig. 10b. The effect of devitrification at a temperature of 550°C is shown in Fig. 10c, after which the coating appears almost completely crystalline with mixture of large (> 1 μm) and small (≈0.1 μm) grains, and a grain boundary phase.

3.3. Optical properties of sol-gel derived coatings

The calculated values of refractive index, band gap and Urbach energy obtained for the TeO₂-TiO₂ films prepared in this work are listed and compared with values obtained by other workers for conventionally prepared tellurite glasses in Table I. From these data, it can be

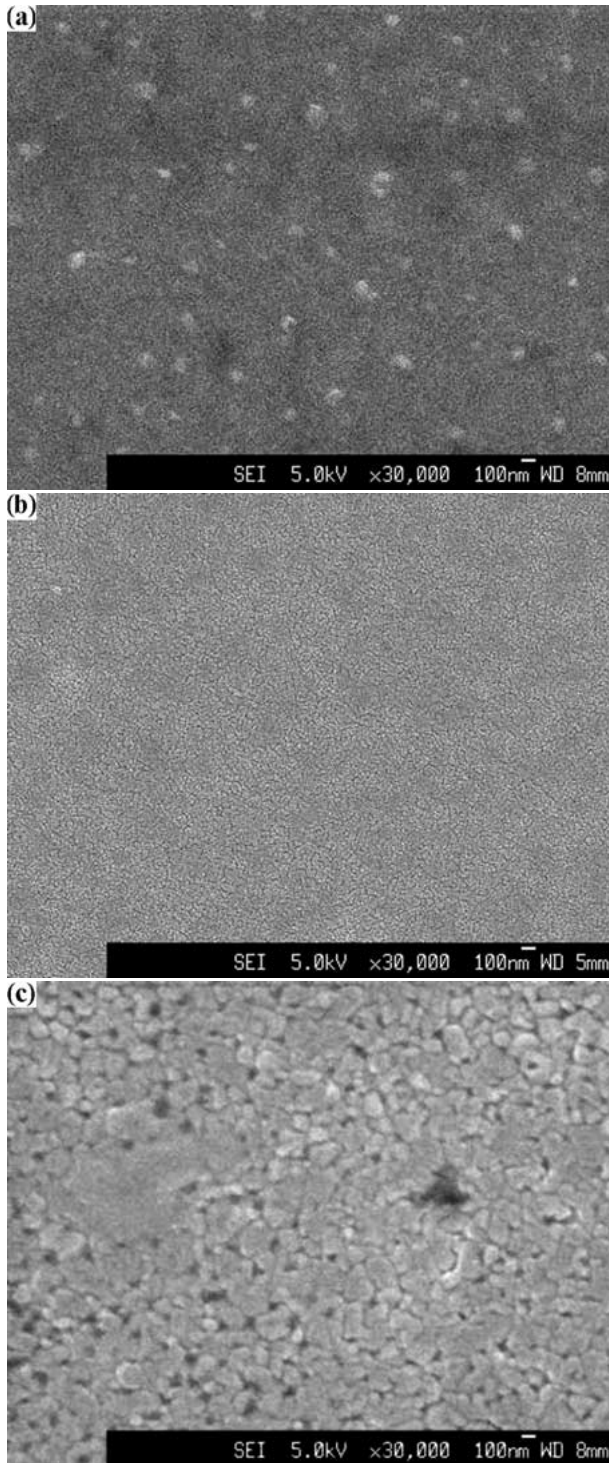


Figure 10 FEG-SEM photomicrographs of microstructure of coating films after heat treatment to (a) 300°C, (b) 450°C and (c) 550°C.

seen that the values obtained from the principal optical parameters are similar for both sol-gel and conventionally prepared tellurite systems. The increase in refractive index (for comparable wavelength) compared to conventionally melted TeO_2 is consistent with the higher refractive index of TiO_2 , and polarisability of the transition metal ions [4].

The optical transparency achievable in sol-gel derived thin films of pure TeO_2 is relatively poor, due to the formation of crystalline metallic Te and $\alpha\text{-TeO}_2$ at relatively low temperatures, as identified in previous studies [10]. In contrast, the increased thermal stability toward devitrification afforded by additions of up to

TABLE I Comparison of optical property values obtained in this study and for conventionally melted materials

Material	Refractive index	Band gap	Urbach energy
Sol-gel derived	2.27 @477 nm	3.29 eV	0.24 eV
90 mol% TeO_2 -	2.20 @550 nm		
10 mol% TiO_2	2.19 @679 nm		
(this work)	2.17 @880 nm		
Conventionally melted TeO_2	2.16 @633 nm [8]	3.79 eV [12]	0.07 [12]
TiO_2 Single crystal (anatase)	2.52 @589 nm [25]	3.65 eV [26]	Not applicable
Conventionally melted	2.13 @633 nm [27]	Not reported	Not reported
90 mol% TeO_2 -			
10 mol% TiO_2			

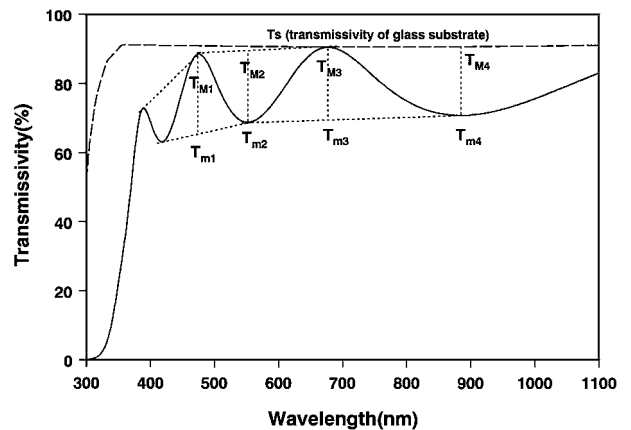


Figure 11 Transmission spectrum of sol-gel derived 0.9 TeO_2 -0.1 TiO_2 thin film, indicating interference maxima and minima values used in the refractive index calculation.

10 mol% TiO_2 allows good quality, dense and transparent thin films to be prepared under appropriate heat treatment conditions. The optimum properties were obtained for heat treatment at 450°C which is sufficient to oxidise any Te phase formed, but below the crystallisation temperature of $\alpha\text{-TeO}_2$ for the system 90 mol% TeO_2 - 10 mol% TiO_2 . The absorption spectra shown in Fig. 11, obtained from approximately 0.5 μm thickness of the sol gel derived coatings, shows good transparency after heating to 450°C. The oscillations and resultant maxima and minima shown in this figure arise from interference effects and are the basis of the refractive index calculation.

The refractive index of the thin film of composition 0.9 TeO_2 -0.1 TiO_2 ($n = 2.19$ at 633 nm) is somewhat higher than that reported for conventionally melted glass of the same composition [27]. However, the values obtained in this study, are more consistent with reported values for pure TeO_2 [8, 12] and TiO_2 [25, 26], and it is believed that the lower values reported for the melt derived material [27] may be attributable to the presence of other oxides derived from the melting crucible in that work. The high value of n obtained in this study suggests that the density of the sol gel derived material was similar to the (assumed maximum) values obtained by conventional melting techniques, with the purity being somewhat higher.

The plot of $(\alpha \cdot h\nu)^{1/2}$ as a function of photon energy used in the calculation of the band gap (E_g) by

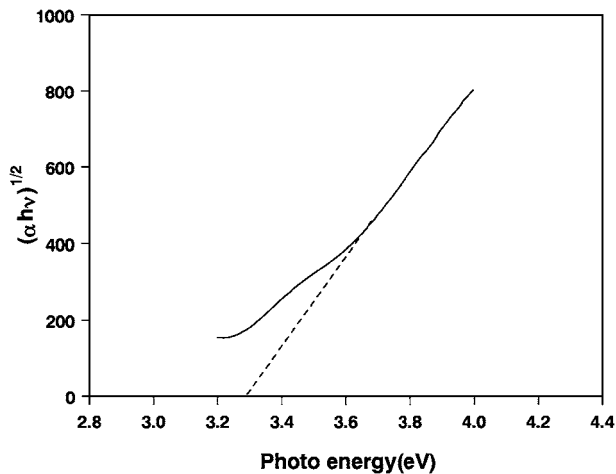


Figure 12 Plot of $(\alpha \cdot hv)^{1/2}$ as a function of photon energy, indicating linear extrapolation used to obtain band gap (E_g).

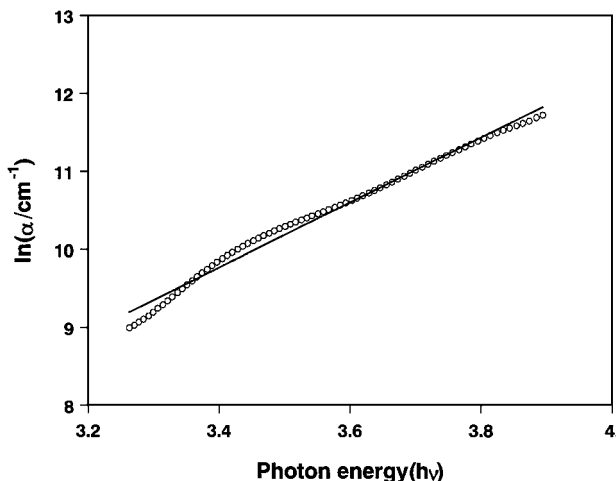


Figure 13 Plot of absorption coefficient ($\ln \alpha$) as a function of photon energy, illustrating line of best fit used to calculate Urbach energy (E_e).

extrapolation is shown in Fig. 12, with the plot of $(\ln \alpha)$ as a function of photon energy from (the slope of) which the Urbach energy value (E_e) was obtained shown in Fig. 13. Both plots show the anticipated linear behaviour and allow reasonable confidence in the results. The reduction in band gap and increase in Urbach energy in comparison with pure TeO_2 shown in Table I are both consistent with an increase in the number of non bridging oxygens [28]. However, these changes are relatively small and are suggestive that the TiO_2 acts as an intermediate rather than network modifier in the TeO_2 glass network, which is consistent with the ionic field strength for the Ti cation [29]. The refractive index value 10 plotted as function of wavelength in Fig. 14.

3.4. Stability of sol-gel derived coatings

The coatings obtained from the TeO_2 - TiO_2 compositions after heat treatment were found to exhibit long term, stability under ambient conditions. No changes in optical properties or microstructure have been observed in the films after storage for 12 months in the laboratory. However, it was found that the precursor solutions (but not pure alkoxides) exhibited limited stability of around 1 month, even when stored in sealed containers with the wetting and coating behaviour of both the single and mixed alkoxide solutions based on

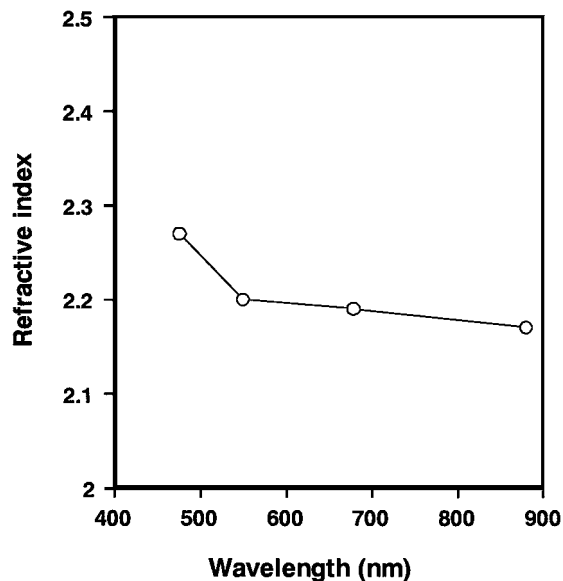


Figure 14 Plot of calculated refractive index values against wavelength for the sol-gel derived 0.9TeO_2 - 0.1TiO_2 films.

tellurium ethoxide being impaired after storage. The mechanisms responsible for this degradation have not been identified.

4. Conclusions

Sol-gel processing routes have been used to prepare optically transparent thin films in the system TeO_2 - TiO_2 , with the calculated refractive index, band gap and Urbach energy values for these films being consistent with the values obtained both in other studies of conventionally melted glasses in this system and from predictions based on the normal behaviour of these oxides in other crystalline and amorphous systems.

The stabilising additives used allowed the formation of thin films for a range of compositions in the system TeO_2 - TiO_2 , although crystallisation of the TiO_2 component occurred on heat treatment when addition levels above approximately 10 mol% TiO_2 were used. It is believed that this devitrification is due to chemical segregation effects associated with the formation of a metallic tellurium phase by reduction of the partially hydrolysed tellurium alkoxide precursor at low temperatures.

It would be anticipated on the basis of the results presented here and previous studies of glasses of similar composition that these materials would be promising candidates for the fabrication of a range of optical devices, with the sol-gel processing route developed in this study offering an attractive route for the fabrication of such materials into device structures.

References

1. P. PRASAD, in "Ultrastructure Processing of Advanced Materials," edited by D. Uhlmann and D. Ulrich (John Wiley & Sons, New York, 1992) p. 461.
2. A. J. IKUSHIMA, *J. Non-Cryst. Solids* **178** (1994) 1.
3. T. WADA, S. YAMADA and Y. MATSUOKA, *Spring Proceedings in Physics* **36** (1989) 292.
4. M. E. LINES, *J. Appl. Phys.* **69** (1991) 6876.
5. E. M. VOGEL, M. J. WEBER and D. M. KORL, *Phys. Chem. Glasses* **32** (1991) 231.
6. R. A. EL-MALLAWANY, *J. Appl. Phys.* **72** (1992) 1774.

7. M. IMAOKA, in "Advances in Glass Technology," edited by Am. Ceram. Soc. (Plenum Press, New York, 1962) p. 149.
8. S. KIM, T. YOKO and S. SAKKA, *J. Amer. Ceram. Soc.* **76** (1993) 2486.
9. S. N. B. HODGSON and L. WENG, *J. Sol Gel Sci. and Tech.* **18** (2000) 145.
10. *Idem.*, *J. Non Cryst. Solids* **276** (2000) 195.
11. R. SWANEPOEL, *J. Phys. E: Sci. Instrum.* **6** (1983) 1214.
12. S. K. J. AL-ANI, C. A. HOGARTH and R. A. EL-MALAWANY, *J. Mater. Sci.* **20** (1985) 661.
13. M. LOVELL, A. AVERY and M. VERNON, "Physical Properties of Materials" (Van Nostrand Reinhold, New York, 1976).
14. M. MALIK and C. HOGARTH, *J. Mater. Sci.* **25** (1990) 713.
15. N. CHOPRA, A. MANSINGH and G. CHADHA, *J. Non-Cryst. Solids* **126** (1990) 194.
16. A. ABDEL-KADER, A. HIGAZY and M. ELKHOLY, *J. Mater. Sci.: Mat. in Electron.* **2** (1991) 204.
17. M. HASSAN and C. HOGARTH, *J. Mater. Sci.* **23** (1988).
18. M. CALZADA, R. SIRERA, F. CARMONA and B. JIMENEZ, *J. Amer. Ceram. Soc.* **78** (1995) 1802.
19. Joint Committee for Powder Diffraction Standards Files, Pub. JCPDS International Centre for Diffraction standards, File No. 36-1452, Metallic Tellurium, (1993).
20. D. C. BRADLEY, R. C. MEHROTRA and D. P. GAOR, "Metal Alkoxide" (Academic Press Inc., London, 1978) p. 191.
21. S. M. TRACEY, S. N. B. HODGSON, A. K. RAY and Z. GHASSEMLOOY, *J. Mat. Proc. Tech.* **77** (1998) 86.
22. J. C. SABADEL, P. ARMAND and D. CACHAU-HERREILLAT, *J. Solid State Chemistry* **132** (1997) 411.
23. N. MOCHIDA, K. TAKAHASHI, K. NAKATA and S. SHIBUSAWA, *Yogyo-Kyokai-shi* **86** (1978) 317.
24. M. ARNAUDOV, V. DIMITROV, Y. DIMITRIEV and L. MARKOVA, *Mat. Res. Bull.* **17** (1982) 1121.
25. W. D. KINGERY, H. K. BOWEN and D. R. UHLMANN, "Introduction to Ceramics," 2nd ed. (John Wiley, New York, 1976) p. 669.
26. M. HILGENDORFF and V. SUNDSTROM, *J. Phys. Chem. B* **102** (1998) 10505.
27. H. YAMAMOTO, H. NASU and J. MATSUOKA, *J. Non-Cryst. Solids* **170** (1994) 87.
28. M. HASSAN, W. KHELIF and C. HOGARTH, *J. Mater. Sci.* **24** (1989) 1607.
29. L. PYE, H. STEVENS and W. LACOURSE (eds.), "Introduction to Glass Science" (Plenum Press, New York, 1972).

*Received 30 November 2000
and accepted 16 January 2002*